Shear Strength and Morphological Study of Polyurethane-OMMT Clay Nanocomposite Adhesive Derived from Vegetable Oil-Based Constituents

Swarnalata Sahoo[1,2]*, Hemjyoti Kalita[1], Smita Mohanty[1,2] and Sanjay Kumar Nayak[1,2]

[1]Central Institute of Plastic Engineering and Technology, Chennai, Tamil Nadu 600032, India

[2]Laboratory for Advanced Research in Polymeric Materials (LARPM), CIPET, Bhubaneswar 751024 India and Chennai, Tamil Nadu 600032, India

ABSTRACT: In the current work, we have synthesized vegetable oil-based polyurethane-OMMT clay nanocomposite (PUNC) adhesive with the incorporation of different wt% of organically modified nanoclay (1 to 5 wt%) into the biobased polyurethane (PU) matrix through *in-situ* polymerization process via ultrasonication method. At the initial stage, PU adhesive was prepared using polyol and partially biobased aliphatic isocyanate, wherein polyol was derived from the transesterified castor oil using ethylene glycol. The formation of PU and PUNC adhesive was confirmed using Fourier transform infrared (FTIR) spectroscopy analysis. The tensile strength of PU with different wt% of nanoclay was determined and the analysis showed that the loading of 3 wt% of nanoclay within the PU matrix showed better performance as compared to the others. Furthermore, shear strength of PU and PUNC (3 wt% nanoclay) adhesives were determined using lap shear test, in which PUNC adhesive showed higher adhesive strength at 70 °C. Subsequently, the dispersibility of OMMT nanoclay within the PU matrix along with exfoliation and amorphous structure was confirmed through wide angle X-ray diffractometer (WAXD) and transmission electron microscopy (TEM) analysis. The phase separation structure was analyzed using dynamic mechanical analysis (DMA). The analysis revealed that with the addition of organically modified nanoclay in the PU matrix, the glass transition temperature (T_g) of the damping curve was shifted towards higher temperature.

KEYWORDS: Biobased raw material, composite material, green strength, gel time, DMA

1 INTRODUCTION

Nowadays, the development of polyurethane nanocomposite adhesive from castor oil is utilized in a wide range of applications, like woodworking, packaging, furniture building and many others, because it has many potential advantages, including high shear strength, flexibility, reactivity and high thermal stability, etc. Wang and Pinnavia have reported that the incorporation of nanoclay within the polymer matrix will enhance the gas and vapor barrier properties of polymeric adhesive, which can be used as a packaging film application [1]. In addition to the above study, there have been several other accounts of the development of polyurethane-clay nanocomposites in the literature [2–7]. Moreover, with respect to polymer

nanocomposite, morphology, which is a branch of life science that deals with the study of structural forms of nanofiller in the polymer matrix, is of great importance. It has been known for about a century that the incorporation of nanofillers into the polymer matrix has strong effects on the properties of polymeric materials, presenting advanced properties compared to the pristine polymer [8–14].

Montmorillonite is a type of natural clay mineral which has a layered structure. It consists of two silica tetrahedral sheets sandwiching an edge-shared octahedral sheet of either aluminum or magnesium hydroxide. Akelah *et al.* [15] have reported that there are some hydrophilic cations such as Na^+ or K^+ ions residing in the gallery, which can possibly be exchanged by other cations. To overcome the incompatibility problem between polymer and silicate, the modification of montmorillonite is required using organic cations such as alkyl ammonium ions. Organically modified nanoclay-based biobased PUNC

Corresponding author: sahoo.swarnalata@gmail.com

adhesives have recently gained importance due to the great potential that the superior properties of the base (polymer) materials have compared to other polyurethane composites. These properties include high dimensional stability, enhanced mechanical properties and better flame retardant properties [16–19]. In addition, polyurethanes are versatile polymer materials with a wide range of applications, such as coatings, adhesives, elastomers, and foams, that can be utilized to meet broadened demands in today's research; but they have some disadvantages such as low mechanical and thermal stability and low adhesion properties. To control these disadvantages, in recent years a great effort has been directed towards vegetable oil-based polyurethane with the incorporation of OMMT nanoclay [1, 20, 21]. Vegetable oil is a renewable resource which removes unwanted odors and reduces toxicity in the environment. Renewable resource technology dispels unwanted odors and tends to the needs of industry and research areas by extending excellent performance and high levels of use. Hence, the components of polyurethanes, such as polyol and the isocyanate derived from vegetable oil, offer benefits which compensate various applications in adhesion and coating technology. Moreover, the prepared polyurethane using the biobased components reduces the toxicity of low volatile organic compounds (VOCs), thus avoiding environmental pollution [22–27]. Gurunathan *et al.* [25] synthesized a new biocomposite material based on castor oil linked waterborne polyurethane nanocomposite reinforced with various percentages of organically modified nanoclay C30B, and studied in depth the effect of nanoclay on the PU matrix. They found high performance-based nanocomposite material, which can have a significant effect on the development of sustainable green material with superior performance for various applications.

In polymer nanocomposite, morphology is one of the main contributors to various physical properties such as transparency, permeability, elasticity, adhesive strength and tensile strength. Moreover, morphology describes the characteristics of the phase structure, including the domain sizes, shapes, and their spatial distribution. Morphology, together with the interfacial forces between the phases, determines the final properties of the blend. Morphology is in turn determined by the intrinsic properties of the components and by the conditions under which the blend is prepared. Therefore, a deeper investigation of morphology will result in a better understanding of the laws governing the preparation of polymeric blend materials. For this work, imaging techniques were chosen as the study tools; hence they provide direct views of the structure of the samples.

The aim of this research work was to synthesize biobased polyurethane-OMMT clay nanocomposite (PUNC) adhesive from vegetable oil. The present work focuses on the adhesive strength and morphological characteristics of PU adhesive with the incorporation of different wt% of nanoclay. The formation of PU and PUNC adhesive was confirmed through FTIR analysis. Subsequently, the tensile strength of PU adhesive film with the loading of different wt% of nanoclay was determined. The corresponding adhesive strength at different temperature media was determined using lap shear test. The confirmation of good dispersion of layer silicate into the PU matrix was obtained by WAXD and TEM analysis. In addition, DMA analysis was performed to confirm the phase separation structure.

2 EXPERIMENTAL

2.1 Materials

The vegetable oil, castor oil and ethylene glycol were purchased from SD Fine Chem, Kolkata; partially biobased aliphatic isocyanate (Tolonate™ X FLO 100) was kindly donated by Vencorex, France; the catalyst dibutyl tin dialurate (DBTDL) was purchased from Sigma-Aldrich, Germany; tetrahydrofuran (THF) was supplied by Fisher Scientific, USA; and OMMT (Closite 30B) nanoclay was purchased from Southern Clay Products, USA.

2.2 Preparation of Polyurethane Nanocomposite

The polyurethane nanocomposite (PUNC) sample was prepared using OMMT nanoclay in the PU matrix. Initially, the PU was prepared using castor oil modified polyol and partially biobased aliphatic isocyanate of NCO:OH molar ratio (1.3:1) using addition polymerization process as reported in our earlier literature paper [28]; wherein the castor oil modified polyol was prepared by the transesterfication process using castor oil and ethylene glycol. At the next stage, different amounts of organically modified (1 to 5 wt%) nanoclay were dried and then separately mixed in THF solution with constant stirring. Then the clay solution was sonicated for 50 min to minimize the agglomeration. Then, the solution was gradually added to the PU solution with continuous stirring for 15 min in the presence of N_2 atmosphere. Further, the prepared solution was then poured into the cleaned glass plate to obtain film sample. A schematic representation of the complete synthesis of PUNC is shown in Figure 1.
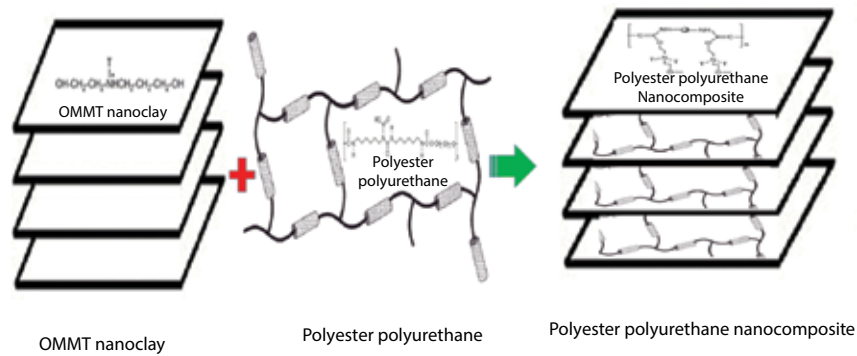
Figure 1 Schematic representation of synthesis of PUNC.

3   CHARACTERIZATIONS

3.1   Fourier Transform Infrared Spectroscopy (FTIR) Analysis

The spectra of PU and PUNC adhesive films were recorded using a FTIR spectrometer (Nicolet 6700, Thermo Scientific, USA) equipped with an attenuated total reflectance (ATR) attachment with 64 scans over the wavelength range of 4000 to 400 cm^{-1}.

3.2   Tensile Strength

Tensile properties of PU and PUNC adhesive films were determined using a universal testing machine (model 3382, Instron, UK) in accordance with ASTM D638 standard. Film samples of dimensions 165 × 13 × 3 mm were strained at a crosshead speed of 5 mm/min and gauge length of 50 mm.

3.3   Preparation of Wood Specimens

As per the test requirements, the wood specimens were cut into 300 × 25 × 3 mm^3 size strips and after that the wood specimens were polished using 60-grit sandpaper.

3.4   Wood Bonding and Testing

The adhesive solution was applied on both the substrates of wood of 0.1 mm thickness of area 25 × 30 mm^2 by using a brush. A load of 2.5 kg was placed over the contact area of the substrates and left overnight. After that the joint specimens were kept at different temperature media for 10 days, such as at room temperature 30 °C, 50 °C, 70 °C, and 100 °C, and at relative humidity of 50 ± 2% respectively. Each joint specimen was tested for the lap shear strength using a universal testing machine as per the standard ASTM D906-82 with a loading rate of 600 lb/min [21]. Five replicate samples were taken for each test and the data reported are the average of five samples.

3.5   Dynamic Mechanical Analysis (DMA)

To analyze the phase separation structure and mechanical properties of PU with and without the incorporation of nanoclay, DMA technique (Q800, TA Instruments) was used at three-point tensile mode. The outcomes, such as storage modulus and damping (tan δ) properties as a function of temperature at a frequency 1 Hz, have been focused on to observe the phase separation structure. The temperature range applied in the present work varied from −100 °C to 100 °C, with a heating rate of 10 °C/min.

3.6   Wide Angle X-ray Diffraction (WAXD) Analysis

Wide angle X-ray diffraction analysis was used to analyze the interlayer gallery spacing of nanoclays in the nanocomposites using an X'Pert MPD diffractometer (Philips, Japan) with graphite monochromator and a Cu Kα radiation source operated at 40 kV and 30 mA.

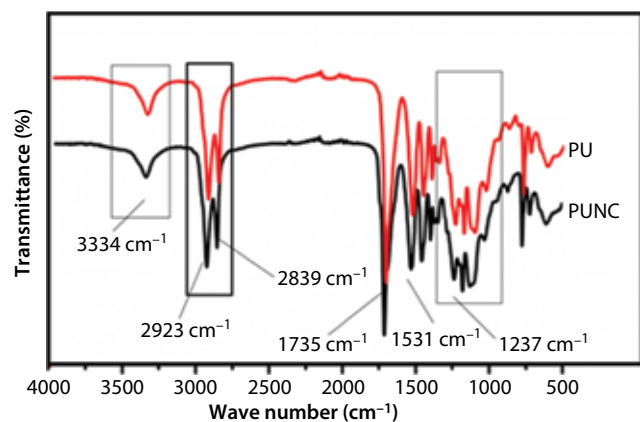## 3.7   Transmission Electron Microscopy (TEM) Analysis

The TEM analysis of thin sectioned samples of PUNC was carried out using a transmission electron microscope by JEOL, Japan, with a scanning range of 0.2 nm under a voltage range of 40–120 kV, and the samples were prepared using a microtome with thickness setting of 85 nm.

4   RESULTS AND DISCUSSION

4.1   FTIR Analysis

The IR spectra of PU and PUNC adhesive containing 3 wt% nanoclay are recorded in Figure 2. As

evidenced from Figure 2, the characteristic absorption peaks were observed at 3334 cm^{-1} due to the presence of urethane stretching. The absence of isocyanate peak at 2260 cm^{-1} indicated the completion of reaction between soft segment (OH group) and hard segment (NCO group) in both PU and PUNC adhesive. The bands observed at 2923–2839 cm^{-1}, 1735 cm^{-1}, and 1237 cm^{-1} were attributed to –CH$_2$ stretching frequencies, carbonyl urethane stretching and coupled C-N and C-O stretching respectively. Hence, the above analysis showed similar IR spectra in PU and PUNC adhesive. No differences in position of band assignments were observed in PU and PUNC adhesive, except for a change in band intensity. This was obtained in accordance with the preparation of PUNC adhesive by other groups and formation of more numbers of H-bond s between clay and PU. However, the band position of the distinct functional group of the PU was identical to those of PUNC. This fact has also been reported by other researchers, which confirmed that the presence of silicate layers does not change the chemical structure of polyurethane [29]. To assure the chemical interaction between nanoclay and the individual components of polyurethane, the FTIR study confirmed the complete reaction obtained on the PUNC surface.

4.2 Mechanical Properties of PU and PUNC Adhesive Films

The mechanical properties in terms of tensile strength, elongation at break and Young's modulus of PUNC adhesive film were analyzed and tabulated in Table 1. The data showed a gradual increase in mechanical properties with the increase in wt% of nanoclay. Furthermore, analysis has also shown that when the clay content was 3%, the tensile strength was higher than that of pure PU. This enhancement of tensile strength is ascribed to the resistance exerted by the clay itself as well as the orientation and high aspect ratio of the clay layers. However, the incorporation of nanoclay beyond 3 wt% decreased the tensile properties, which might be due to the aggregation of nanoclay particles which resulted in the predominance of filler-filler interaction over the polymer-filler interaction [30]. Hence, PUNC (3 wt%) nanoclay was chosen as the optimized nanocomposite for further comparative studies in the following sections. Furthermore, it has also been found that the tensile strength and Young's modulus of PUNC adhesive film are 1.49 and 1.84 times higher than those of PU adhesive film with the incorporation of 3 wt% of OMMT nanoclay within the matrix. This behavior is primarily due to the presence of nanoclay, which acts as a reinforcing agent that assists in stress transfer at the interface. It is also assumed that the intercalation of polyurethane chains inside the nanoclay layers increases the surface area between the nanoclay and polymer chains, which results in the stronger polar interactions between the silicate layer and polymer chain. These increased polar interactions are responsible for the improvement of tensile strength of the PUNC adhesive film. Moreover, the elongation at break of PUNC adhesive film was found to decrease as compared with PU adhesive film. This is possibly due to the higher crosslinking which occurs between

Figure 2 FTIR spectra of PU and PUNC adhesives.

Table 1 Mechanical properties of PU and PUNC adhesive films.

Type of adhesive	Tensile strength (MPa)	Elongation at break (%)	Young's modulus (Mpa)
PU	6.3 ± 1.26	558 ± 1.77	13.3 ± 0.84
PUNC (1 wt% nanoclay)	8.1 ± 1.62	691 ± 1.91	15.2 ± 1.34
PUNC (3 wt% nanoclay)	9.4 ± 1.85	715 ± 1.95	17.3 ± 1.56
PUNC (5 wt% nanoclay)	9.1 ± 1.82	721 ± 1.97	16.9 ± 0.45

the organic phase of BPU and the inorganic phase of nanoclay.

4.3 Adhesion Strength: Effect of Temperature and Humidity on the Shear Strength of Adhesives

The shear strength values of PU adhesive after the incorporation of 1 to 5 wt% of nanoclay are summarized in Table 2. The results showed the improvement of bonding strength with the increase in clay content. It was found that the integration of 3 wt% of nanoclay throughout the PU matrix showed higher bonding strength, which was chosen as optimum composition because the incorporation of 5 wt% of nanoclay throughout the PU matrix exhibited less shear strength as compared to PU with the incorporation of 3 wt% of nanoclay. This might be due to the aggregation of nanoclay particles, which resulted in the weak interaction of filler-filler over the polymer-filler. Furthermore, the mode of failure was obtained as cohesive failure (CF).

The shear strength, shear strength at break and shear force of PU and PUNC (3 wt% of nanoclay) were determined using a lap shear test, as reported in Table 3. It is observed that the shear strength, shear strength at break and the shear force of wood specimens based on PU and PUNC adhesive increase with the increase in temperature from room temperature to 80 °C; beyond this temperature, the shear strength, shear stress at break and shear force starts decreasing. This is because of the effect of curing due to the generation of heat induced by the higher temperature in which the absorbed heat increased the kinetics of

the reaction to some extent. But at a higher temperature of 100 °C, the deterioration of adhesive strength decreased, due to the formation of amines, carbon monoxide, CO_2, etc., produced by high heat stimulation in the hydrolysis of PU [31]. Hence, it can be concluded that above 100 °C, the materials are formed as unstable adhesive due to the change in cellular and chemical structure in adhesives, but below 70 °C, the developed adhesives are stable [32]. The shear strengths of PU adhesive were found to be 6.95, 8.23, 8.45 and 6.35 Mpa respectively, whereas the shear strengths of PUNC adhesive were found to be 10.35, 11.52, 11.93 and 9.98 MPa respectively, corresponding to the temperatures 30, 50, 70, 100 °C. Hence, it can be concluded that PUNC adhesive shows better adhesion strength over the PU adhesive. This is due to the strong interfacial adhesion bonding between the wood substrates and the PU adhesive containing 3 wt% of nanoclay content, which was induced due to the strong interfacial interaction between the OH groups of OMMT clay with the OH group in wood substrate respectively.

Furthermore, a study was conducted in which the specimens were immersed in water for 24 h, which showed that the humidity did not affect the shear strength of the sample; but after 10 days it had a negligible effect on shear strength, as shown in Table 4. Hence, it can be concluded that the adhesion strength between both wood substrates was much stronger than that of the interface areas where the water molecules were not able to penetrate the surface. This is due to the hygroscopic nature of the wood substrate [33].

Table 2 Adhesion strength (lap shear strength) of PU with the incorporation of different wt% of nanoclay.

Sample code	Wood-Wood bonding strength of BPUNC after 10 days (N/m^2× 10^5)	Mode of failure
PU	51 ± 0.65	CF
PUNC (1 wt% nanoclay)	53 ± 0.42	CF
PUNC (3 wt% nanoclay)	61 ± 0.15	CF
PUNC (5 wt% nanoclay)	59 ± 0.31	CF

Table 3 Lap shear strength data of PU and PUNC adhesives.

Adhesive sample code	Lap shear strength for wood-wood bonding											
	Max. shear force (N)				Shear strength at break (MPa)				Shear strength (MPa)			
	30 °C	50 °C	70 °C	100 °C	30 °C	50 °C	70 °C	100 °C	30 °C	50 °C	70 °C	100 °C
PU	1882	2445	2965	1348	6.3 ± 0.25	7.5 ± 1.4	7.6 ± 01.52	6.19 ± 1.34	6.97 ± 1.35	8.23 ± 1.71	8.45 ± 0.63	6.3 ± 0.45
PUNC	2114	2645	3015	1654	10.1 ± 0.41	10.3 ± 1.9	11.1 ± 1.98	8.95 ± 1.65	10.35 ± 0.62	11.52 ± 1.93	11.9 ± 1.98	9.9 ± 0.65

Table 4 Lap shear strength of PU and PUNC adhesives in presence of humidity.

Adhesive sample code	Lap shear strength (MPa)		
	After one day exposure of joint specimen	After five day exposure of joint specimen	After ten day exposure of joint specimen
PU	6.97 ± 1.54	6.95 ± 0.95	6.91 ± 0.35
PUNC	10.35 ± 1.97	10.34 ± 1.65	10.30 ± 1.71
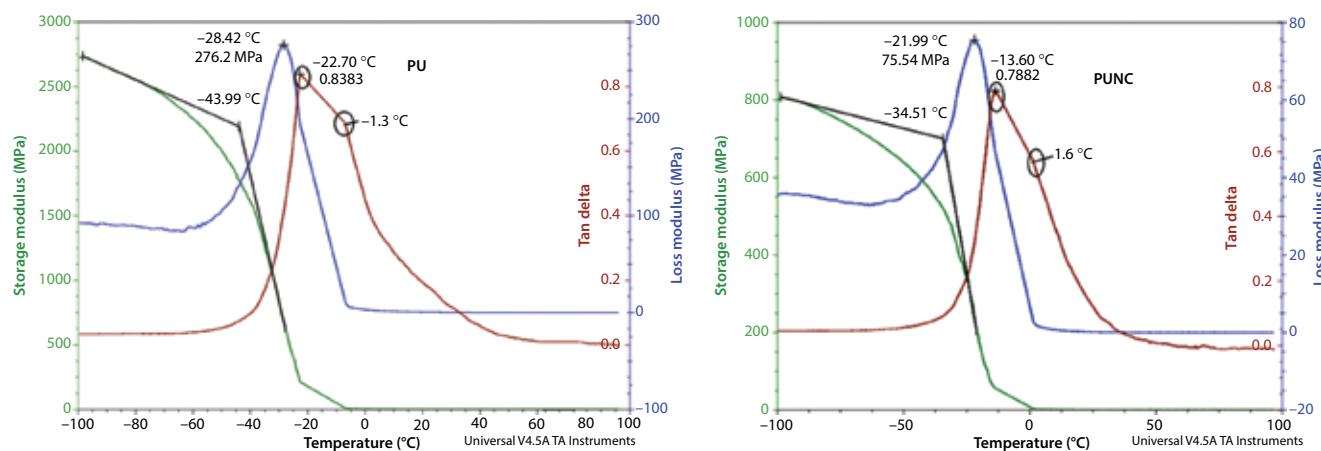
Figure 3 DMA curves of PU and PUNC adhesive films.

4.4 Dynamic Mechanical Analysis (DMA)

To analyze the mechanical and surface properties of PU and PUNC sample, DMA technique was carried out. The outcomes, such as storage modulus (E'), loss modulus (E'') and damping (tan δ) properties, have been focused on to characterize the polymer's ability to store energy and dissipation of energy of a material in terms of recoverable energy. All the outcome parameters were measured as a function of temperature, which depends upon the structure of polyurethane sample.

The storage modulus (E'), loss modulus (E'') and damping (tan δ) versus temperature curves for PU and PUNC are shown in Figure 3. The T_g values due to E' corresponding to PU and PUNC were found to be −38 °C and −28 °C respectively by confirming the onset temperature points of the drop at which the storage modulus started falling during heating to a level of one-thousandth of its initial value. Hence, the lower T_g value of PU than that of PUNC indicated that the molecular segments are less mobile in PU sample [34]. It is also observed that after glass transition, the modulus steadily decreases at the temperature range −50 °C to −10 °C. The presence of hard segment content in PU and PUNC adhesive reduces the modulus due to the interaction between the soft segments. The peak

temperatures at −28.42 °C and −21.99 °C corresponding to PU and PUNC due to E'' indicated the point of maximum chain slippage in a crosslinked system.

The damping curves of PU and PUNC are depicted in Figure 3. It is observed that two damping (tan δ) peaks are present in each curve of PU and PUNC sample corresponding to the glass transition temperature of the soft and hard domain. The T_g values are obtained at −22.3 °C and −1.3 °C for PU sample, as reported in the earlier literature [35], wherein −15 °C and 1.6 °C for PUNC sample represent soft and hard domain. Hence, it can be observed that the T_g of PUNC sample was shifted towards higher temperature due to the existence of strong interaction bonding between clay and PU, which limits the movement of segmental PU chain by forming the phase separation structure on the surface. Kazemabad *et al.* [34] reported that the T_g of soft and hard domain for PU ranges from −60 °C to 128 °C, wherein negative temperature and positive temperature were obtained due to soft and hard domain respectively. However, in the present work the T_g of both domains of PU exhibits negative value. This might be due to the high compatibilization of both the domains in the synthesized PU. However, with the incorporation of nanoclay within the PU matrix, the T_g values shifted towards high values due to an increase in restriction of segmental mobility of polyurethane

chain, confirmed by the formation of more numbers of H-bonds between the hydroxyl groups of nanoclay and urethane groups of PU [36]. The above results are in good agreement with that of the FTIR analysis discussed earlier. Hence, it can be confirmed by the above study that PUNC exhibits higher crosslinking density.

4.5 Wide Angle X-ray Diffraction (WAXD) Analysis

The WAXD diffraction pattern was used in order to investigate the specific dispersion of OMMT clay throughout the PU matrix and the interlayer spacing between the PU and PUNC sample represented in Figure 4. A strong diffraction peak appeared at $2\theta = 5.09°$ for OMMT nanoclay. The disappearance of this peak at $2\theta = 5.09°$ in the PUNC sample confirmed the strong interaction of clay and PU matrix. This indicated the increase in distance from a certain plane in one layer corresponding to another layer of the plane. Hence, the diffraction was observed and the basal of the polymer can be calculated by using Bragg's law: $d \sin \theta = n\lambda$. The diffraction peaks of PU and PUNC sample were found to be $19.2°$ and $20.25°$ with basal spacing 4.3 and 4.5 nm respectively. Thus, the higher value of basal spacing indicates that the silicate layers in polyurethane molecular chains are exfoliated and absence of intercalation was observed. This indicated that the galleries of clay layers expanded in the PUNC sample [37].

4.6 Transmission Electron Microscopy (TEM) Analysis

To investigate the spatial distribution of OMMT clay (Closite 30B) into the PU matrix, TEM analysis was done and is presented in Figure 5. Small exfoliated tactoids of nanoclay with homogeneous dispersed structure inside the PU matrix were observed. This may be attributed to the strong interaction between the hydrogen bonding between the carbonyl groups in PU and hydroxyl groups in OMMT nanoclay. Similar results have been reported in previous studies [28]. In addition, the presence of exfoliated structure and absence of intercalated structure of nanoclay in PU matrix has been observed. As observed from WAXD analysis, the exfoliation of nanoclay was again confirmed here. It has also been observed that the tactoid dark spots with almost similar diameter over the matrix indicated the homogeneous distribution of nanoclay [38].

5 CONCLUSIONS

We have synthesized vegetable oil-based PUNC adhesive with the incorporation of different wt% of nanoclay (1 to 5 wt%) within the PU matrix. The formation of PU and PUNC adhesive was confirmed through FTIR analysis. The incorporation of 3 wt% of nanoclay within the PU matrix was optimized through mechanical and adhesion strength test. Furthermore,
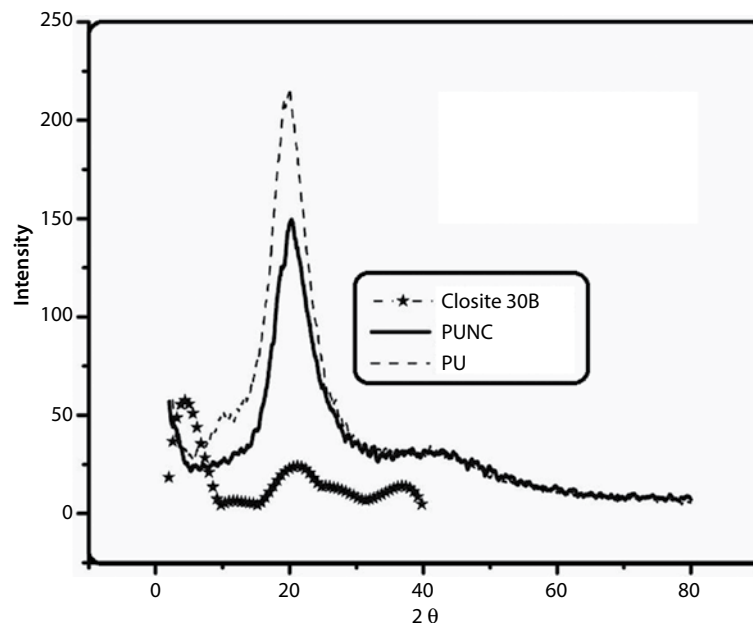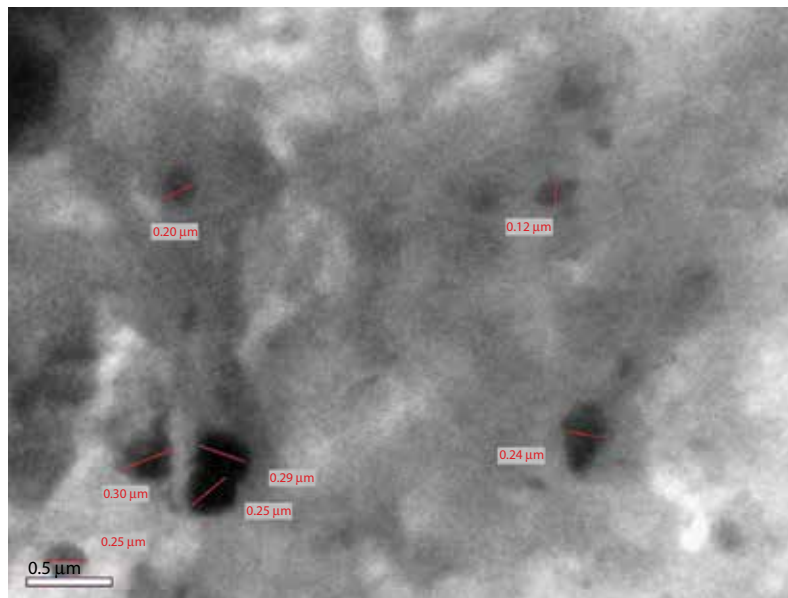

Figure 4 WAXD analysis of PU and PUNC adhesive films.

Figure 5 TEM analysis of PUNC adhesive film.

the PUNC adhesive showed better adhesion strength over the PU adhesive and exhibited higher resistance at the temperature range from 30 °C to 70 °C. It has also been ascertained that the adhesive showed good resistant to moisture. The morphological analysis of PU and PUNC was carried out through WAXD and TEM analysis. The good dispersion of nanoclay into the polymer matrix was verified by TEM analysis. It is clearly demonstrated that the nanoclay layers were well dispersed and intercalated within the polyurethane matrix. In addition, the phase separation structure was obtained by DMA analysis due to the occurrence of phase domains in the resulting PU adhesive film.

ACKNOWLEDGMENT

Conflict of interest: The authors declare that they have no conflict of interest.

REFERENCES

1. Z. Wang and T.J. Pinnavia, Nanolayer reinforcement of elastomeric polyurethane. *Chem. Mater.* **10**, 3769–3771 (1998).
2. C. Zilg, R. Thomann, R. Mülhaupt, and J. Finter, Polyurethane nanocomposites containing laminated anisotropic nanoparticles derived from organophilic layered silicates. *J. Adv. Mater.* **11**, 49–52 (1999).
3. K.J. Yao, M. Song, D.J. Hourston, and D.Z. Luo, Polymer/layered clay nanocomposites: 2 polyurethane nanocomposites. *Polymer* **43**, 1017–1020 (2002).
4. T.K. Chen, Y.I. Tien, and K.H. Wei, Synthesis and characterization of novel segmented polyurethane/clay nanocomposite via poly(ε-caprolactone)/clay. *J. Polym. Sci: Polym. Chem.* **37**, 2225–2233 (1999).
5. T.K. Chen, Y.I. Tien, and K.H. Wei, Synthesis and characterization of novel segmented polyurethane/clay nanocomposites. *Polymer* **41**, 1345–1353 (2000).
6. Y.I. Tien and K.H. Wei, Hydrogen bonding and mechanical properties in segmented montmorillonite/polyurethane nanocomposites of different hard segment ratios. *Polymer* **42**, 3213–3221 (2001).
7. Y.I. Tien and K.H. Wei, High-tensile-property layered silicates/polyurethane nanocomposites by using reactive silicates as pseudo chain extenders. *Macromolecules* **34**, 9045–9052 (2001).
8. E.P. Giannelis, Polymer layered silicate nanocomposites. *Adv. Mater. Weinheim* **8**, 29–35 (1996).
9. E.P. Giannelis, R. Krishnamoorti, and E. Manias, Polymer-silicate nanocomposites: Model systems for confined polymers and polymer brushes. *Adv. Polym. Sci.* **138**, 107–147 (1999).
10. Y. Kojima, A. Usuki, M. Kawasumi, A. Okada, Y. Fukushima, T. Kurauchi, and O. Kamigaito, Mechanical properties of nylon 6-clay hybrid. *J. Mater. Res.* **8**, 1185–1189 (1993).
11. D. Schmidt, D. Shah, and E.P. Giannelis, New advances in polymer/layered silicate nanocomposites. *Curr. Opin. Solid State Mater. Sci.* **6**, 205–212 (2002).
12. M. Alexandre and P. Dubois, Polymer-layered siliate nanocomposites: preparation, properties and uses

of a new class of materials. *Mater. Sci. Eng.* **28**, 1–63 (2000).

13. P.C. LeBaron, Z. Wang, and T. Pinnavaia, Polymer-layered silicate nanocomposites: An overview. *Appl. Clay Sci.* **15**, 11–29 (1999).

14. M. Modesti, A. Lorenzetti, S. Besco, D. Hrelja, S. Semenzato, R. Bertani, and R.A. Michelin, Synergism between flame retardant and modified layered silicate on thermal stability and fire behaviour of polyurethane nanocomposite foams. *Polym. Degrad. Stab.* **93**, 2166–2171 (2008).

15. A. Akelah, P. Kelly, S. Qutubuddin, and A. Moet, Synthesis and characterization of 'epoxyphilic' montmorillonites. *Clay Minerals* **29**, 169–178 (1994).

16. S. Chuayjuljit, A. Maungchareon, and O. Saravari, Preparation and properties of palm oil-based rigid polyurethane nanocomposite foams. *J. Reinf. Plast. Compos.* **29**, 218–225 (2010).

17. S.K. Wai, A. Sahrim, and S.A. Zubir, Synergism between flame retardant and phosphonium salt modified layered silicate on properties of rigid polyurethane foam nanocomposite. *Adv. Mater. Res.* **501**, 8–12 (2012).

18. S. Semenzato, A. Lorenzetti, M. Modesti, E. Ugel, D. Hrelja, and S. Besco, A novel phosphorus polyurethane FOAM/montmorillonite nanocomposite: Preparation, characterization and thermal behaviour. *Appl. Clay Sci.* **44**, 35–42 (2009).

19. L. Song, Y. Hu, Y. Tang, R. Zhang, Z. Chen, and W. Fan, Study on the properties of flame retardant polyurethane/organoclay nanocomposite. *Polym. Degrad. Stab.* **87**, 111–116 (2005).

20. N. Nurfatmah Pz Nik Pauzi, R.A. Majid, M. Haziq Dzulkifli, and M. Yazid Yahya, Development of rigid bio-based polyurethane foam reinforced with nanoclay. *Compos. Part B* **67**, 521–526 (2014).

21. K.P. Somania, S.S. Kansaraa, N.K. Patel, and A.K. Rakshita, Castor oil based polyurethane adhesives for wood-to-wood bonding. *Int. J. Adhes. Adhes.* **23**, 269–275 (2003).

22. B.B.R. Silva, R.M.C. Santana, and M.M.C. Forte, A solventless castor oil-based PU adhesive for wood and foam substrates. *Int. J. Adhes. Adhes.* **30**, 559–565 (2010).

23. J.O. Metzger and M. Eissen, Concepts on the contribution of chemistry to a sustainable development. Renewable raw materials. *C. R. Chim.* **7**, 569–581 (2004).

24. D.E. Packham, Adhesive technology and sustainability. *Int. J. Adhes. Adhes.* **29**, 248–252 (2009).

25. T. Gurunathan, S. Mohanty, and S.K. Nayak, Effect of reactive organoclay on physicochemical properties of vegetable oil-based waterborne polyurethane nanocomposites. *RSC Adv.* **5**, 11524–11533 (2009).

26. F. Zafar, M. Hassan Mir, M. Kashif, E. Sharmin, and S. Ahmad, Microwave assisted synthesis of bio based metallopolyurethaneamide. *J. Inorg. Organomet. Polym. Mater.* **21**, 61–68 (2011)

27. S. Swain, R.A. Sharma, S. Bhattacharya, and L. Chaudhary, Effects of nano-silica/nano-alumina on mechanical and physical properties of polyurethane composites and coatings. *Trans. Electr. Electron. Mater.* **14**, 1–8 (2013).

28. S. Sahoo, H. Kalita, S. Mohanty, and S.K. Nayak, Synthesis of vegetable oil-based polyurethane: A study on curing kinetics behavior. *Int. J. Chem. Kinet.* **48**, 622–634 (2016).

29. M. Rengasamy, K. Anbalagan, S. Kodhaiyolii, and V. Pugalenthi, Castor leaf mediated synthesis of iron nanoparticles for evaluating catalytic effects in transesterification of castor oil. *RSC Adv.* **6**(11), 9261–9269 (2016).

30. M. Rahman, H. Yoo, C. Mi, and H. Kim, Synthesis and characterization of waterborne polyurethane/clay nanocomposite – Effect on adhesive strength. *Macromol. Symp.* **249–250**, 251–258 (2007).

31. V. Kovačević, D. Hace, M. Bravar, and D.Stanojević, Correlation between mechanical and chemical properties of polyurethane compounds under ageing conditions. *Polym. Degrad. Stab.* **24**, 349–360 (1989).

32. T. Malavašič, N. Černilec, A.Mirčeva, and U. Osredkar, Synthesis and adhesive properties of some polyurethane dispersions. *Int. J. Adhes. Adhes.* **12**, 38–42 (1992).

33. K. Haji Badri, A. Helmi Ujar, Z. Othman, and F. Hani Sahaldin, Shear strength of wood to wood adhesive based on palm kernel oil. *J. Appl. Polym. Sci.* **100**, 1759–1764 (2006).

34. A. Eceiza, M.D. Martin, K. De La Caba, G. Kortaberria, N. Gabilondo, M.A. Corcuera, and I. Mondragon, Thermoplastic polyurethane elastomers based on polycarbonate diols with different soft segment molecular weight and chemical structure: Mechanical and thermal properties. *Polym. Eng. Sci.* **48**(2), 297–306 (2008).

35. S. Benali, G. Gorrasi, L. Bonnaud, and P. Dubois, Structure/transport property relationships within nanoclay-filled polyurethane materials using polycaprolactone-based masterbatches. *Compos. Sci. Technol.* **90**, 74–81 (2014).

36. P. Pandey, S. Anbudayanidhi, S. Mohanty, and S.K. Nayak, Flammability and thermal characterization of PMMA/clay nanocomposites and thermal kinetics analysis. *Polym. Compos.* **33**, 2058–2071 (2012).

37. K. Mahmood Zia, M. Zuber, M. Barikani, A. Jabbar, and M. Kaleem Khosa, XRD pattern of chitin based polyurethane bio-nanocomposites. *Carbohydr. Polym.* **80**, 539–543 (2010).

38. S. Das, P. Pandey, S. Mohanty, and S.K. Nayak, Effect of nanosilica on the physicochemical, morphological and curing characteristics of transesterified castor oil based polyurethane coatings. *Prog. Org. Coat.* **97**, 233–243 (2016).

J. Renew. Mater., Vol. 6, No. 1, January 2018

© 2018 Scrivener Publishing LLC   125